# STH/CFD Coupled Simulation of the Protected Loss of Flow Accident in the CIRCE-HERO Facility

**Pucciarelli Andrea** [1],*[ID], **Galleni Francesco** [1], **Moscardini Marigrazia** [1], **Martelli Daniele** [2] **and Forgione Nicola** [1][ID]

[1] Department of Civil and Industrial Engineering, University of Pisa, 56126 Pisa, Italy; francescog.galleni@dici.unipi.it (G.F.); marigrazia.moscardini@dici.unipi.it (M.M.); nicola.forgione@unipi.it (F.N.)

[2] ENEA, FSN-ING, Brasimone Research Centre, ENEA, 40032 Camugnano (Bo), Italy; daniele.martelli@enea.it

*   Correspondence: andrea.pucciarelli@dici.unipi.it

check for updates

**Abstract:** The paper presents the application of a coupling methodology between Computational Fluid Dynamics (CFD) and System Thermal Hydraulic (STH) codes developed at the University of Pisa. The methodology was applied to the CIRCE-HERO facility in order to reproduce the recently performed experimental conditions simulating a Protected Loss Of Flow Accident (PLOFA). The facility consists of an internal loop, equipped with a fuel pin simulator and a steam generator, and an external pool. In this coupling application, the System code RELAP5 is adopted for the simulation of the internal loop while the CFD code ANSYS Fluent is used for the sake of simulating the pool. The connection between the two addressed domains is provided at the inlet and outlet section of the internal loop; a thermal coupling is also performed in order to reproduce the observed thermal stratification phenomenon. The obtained results are promising and a good agreement was obtained for both the mass flow rates and temperature measurements. Capabilities and limitations of the adopted coupling technique are discussed in the present paper also providing suggestions for improvements and developments to be achieved in the frame of future applications.

**Keywords:** liquid metals; thermal-hydraulics; CIRCE-HERO

## 1. Introduction

Liquid Metal Fast Breeder Reactors (LMFBRs) represent one of the proposed technologies and concepts for the upcoming Generation IV of Nuclear Power Plants. The University of Pisa, in the frame of several programs promoted by the European Union, has joined the common effort for the development of such technologies in the near future. In particular, the development of coupled STH/CFD applications for the analysis of complex thermal-hydraulics phenomena is one of the main commitments of UniPi inside the MYRTE EU H2020 project.

Unlike the LWRs, in fact, LMFBRs consist of several plant components that cannot be reliably modelled adopting STH approaches such as the large reactor pool (see e.g., Ref. [1,2]) or components that may require a three-dimensional approach for a better comprehension of the involved phenomena, as in the case of fuel assemblies adopting wrapped wire rod bundles. As a consequence, stand-alone STH applications are no more suitable for performing thermal-hydraulics analyses addressing the various plant operating and accidental conditions.

Computational Fluid Dynamics (CFD), yet not being considered a reliable tool for licensing matters, usually provides instead valuable estimations for flow conditions in complex three-dimensional environments. In this sense, CFD may be adopted in order to provide better estimations for parameters to be used in STH calculations (see, e.g., Ref. [3]); nevertheless, a more comprehensive approach

is represented by coupled STH/CFD methods that try to obtain the advantages of both approaches without facing the corresponding drawbacks. The main aim is to combine the capabilities of STH codes in predicting flow conditions in complicated pipe systems at limited computational costs, with the capabilities of CFD codes in providing highly detailed predictions of selected regions where complex multi-dimensional phenomena may occur.

In the available literature, examples of the application of coupled STH/CFD codes to liquid metal thermal hydraulics exists, proving the capabilities of the adopted method in predicting the considered experimental conditions. Particularly, several coupled simulations were performed in works by Toti [4–6], aiming at reproducing the behavior of the MYRRHA reactor in postulated conditions, highlighting the advantages with respect to the stand-alone STH and CFD calculations.

In their works, Toti and co-authors also analysed the complex behaviours observed in the E-SCAPE facility (see e.g., Ref. [7]) simulating the lower plenum and the Above Core Structure (ACS) by means of CFD (ANSYS Fluent) calculations while simulating the pipes system with the help of the RELAP5-3D STH code. Improvements with respect to the STH stand-alone approach were observed; in particular, CFD allowed the analysis of the thermal stratification in the ACS which also granted the prediction of an improved pressure distribution in the reactor core. Further works concerning applications of coupled STH/CFD codes to liquid metals were performed at the KTH [8,9]; here, the TALL-3D facility was investigated by means of the CFD code STAR-CCM+ and the STH code RELAP5/Mod3.3. CFD was again considered for one of the large 3D environments components by which the facility is composed: the use of the coupled STH/CFD provided improved results in comparison to the STH stand-alone application, also highlighting the presence of thermal-hydraulic phenomena that could not be spotted without the CFD analysis.

At the University of Pisa, coupling techniques have been developed for the analysis of experimental facilities in order to improve the understanding of phenomena relevant for LMFBRs during both operating and accidental conditions. The coupling methodology, developed in the frame of recent studies [10–15], combines the STH code RELAP5 Mod3.3 with the CFD code ANSYS Fluent; the coupling interface of the simulation is provided by MATLAB scripts. Coupled calculations were performed for the analyses of the NACIE-UP (see e.g., Ref. [11,13]) and the CIRCE-ICE [12,13] and the CIRCE-HERO facilities [10,14,15] experimental campaigns.

Specifically, experimental data regarding postulated PLOFA conditions reproduced in the CIRCE-HERO facility have been recently released by ENEA Brasimone RC [16,17]. In Ref. [14], University of Pisa simulated the experimental conditions neglecting heat exchanges between the internal loop and LBE in the pool. These effects are instead taken into account in the present paper since they proved to be relevant in order to achieve a better reproduction of the experimental data. The present paper reports the results obtained during the preliminary phase of the new simulation campaign to highlight the capabilities of the adopted method and providing suggestions for future developments. Given the objectives of the present Special Issue, the present paper aims at showing the limits and capabilities of the STH/CFD application technique addressing selected operating conditions: the interested reader is referred to the cited papers for more detailed descriptions of each adopted approach. Though providing interesting and promising results, CFD and thus coupled STH/CFD applications are not considered as suitable tools by nuclear licensing agencies. As a consequence, this paper also aims at maintaining open this discussion in the research community, with the objective of paving the way for the proposal of sound Best Practice Guidelines (see, e.g., Ref. [18,19]) that may help in allowing the use of CFD applications for licensing purposes.

## 2. Methods

### 2.1. Considered Experimental Facility

The CIRCE-HERO facility (Figure 1) was designed with the purpose of providing support for the development of pool type LMFBRs [20]. It consists of a large vessel, the pool, 8.5 m high and with a

diameter of 1.2 m filled with LBE (Lead Bismuth Eutectic); inside the pool, an internal loop is allocated. This internal loop consists of several components. The most important are: the Fuel Pin Simulator (FPS), the Fitting Volume (FV) with the Argon Injection System, the Separator and the HERO steam generator. Figure 1 reports the distribution of the main components allocated inside the pool. For a more detailed description of the facility, the reader is referred to [20].
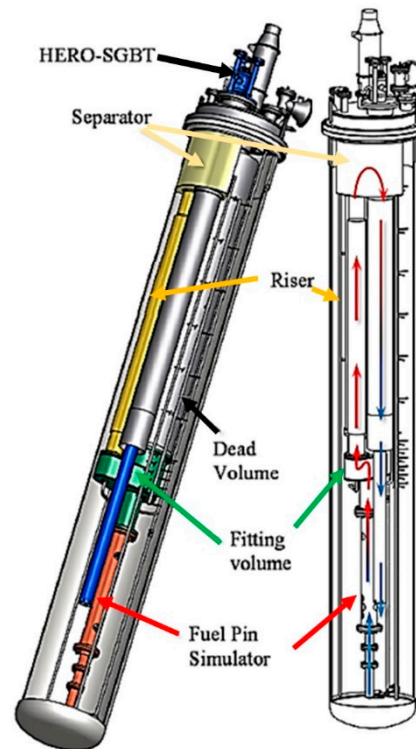


**Figure 1.** CIRCE-HERO facility.

This structure allows the development of natural circulation conditions through the internal loop; circulation may also be enhanced with the injection in the hot leg (Riser) of Argon, which is subsequently separated and collected in the dome at the top of the pool (Separator).

The experimental campaign carried out at ENEA Brasimone RC [21] aimed at reproducing conditions compatible with a postulated PLOFA. In particular, the loss of flow was simulated by reducing the injected Argon mass flow rate and, consequently the LBE flow rate in the hot leg; heat generation in the FPS and water mass flow rate in the steam generator were also changed in accordance with the objective of the experimental campaign.

Table 1 resumes the experimental conditions for the considered test case, highlighting the imposed operating conditions before and after the PLOFA test. This test consists in a progressive decrease of the injected Argon (see also Figure 5 in Section 3 for a detailed trend) in association with a dramatic decrease of the supplied power in about 20 s; the water mass flow rate was reduced too in the same time interval. As a consequence, while at the beginning the fluid flows in the CIRCE loop by mean of mixed/aided circulation, in the final part of the transient a buoyancy-driven flow is instead obtained.

**Table 1.** Considered operating conditions before and after the postulated transient.

| Header | Before | After |
|---|---|---|
| Injected Argon Mass Flow Rate [Nl/s] | 2.73 | 0 |
| HERO Water Mass flow rate [kg/s] | 0.26 | 0.079 |
| Water Inlet Temperature [°C] | 336 | 336 |
| Power at the FPS [kW] | 356 | 20 |

## 2.2. Adopted Model

In the present paper, the CIRCE-HERO facility is simulated adopting a coupled STH/CFD approach. In particular, the CFD code ANSYS Fluent simulates the pool while the STH code RELAP5/Mod3.3 is adopted for the simulation of the internal loop. In addition, the top region of the pool, where the LBE free surface is in contact with Argon, is modeled through RELAP5 to avoid two-phase simulation in the CFD domain. Figure 2 reports a scheme of the considered approach, the location of the interfaces between the regions and the relevant information transferred in their correspondence is reported as well.



**Figure 2.** Coupling scheme and spatial discretization.

This subdivision was chosen, in similarity with other works, in order to exploit the advantages of both codes and, on the other hand, to avoid their drawbacks. In fact, in this way RELAP5 is used for the regions in which the fluid flow may be approximated by a mono-dimensional approach and in the regions where multiphase phenomena occur. ANSYS Fluent, instead, provides predictions for the intrinsically 3-dimensional environment of the pool, dealing with regions in which LBE only is present. The improved modelling capabilities of CFD are thus taken into account for the pool environment only; the introduction of the CFD domain, in fact, dramatically increases the computational cost of the performed calculation and thus must be limited as far as possible. Comparing to STH stand-alone applications, in fact, the coupled STH/CFD calculations are definitively more time consuming; nevertheless, the improved capability of the model and the quality of the information and lessons that can be drawn from the obtained results are often worth the additional computational cost.

In the following, some of the most relevant information about the considered coupling approach is provided. It is worth noticing that, regarding the CFD domain, the inlet/outlet definitions are actually reversed; that is, the outlets of the real facility and the RELAP5 nodalization correspond to the inlets of the CFD computational domain and vice versa.

Concerning the spatial discretization, a non-overlapping approach was adopted: RELAP5 and ANSYS Fluent solve autonomously their corresponding domains and only communicate at some selected boundaries. In particular, fluid-dynamic boundaries are imposed at the FPS inlet and at the HERO-SGBT outlet.

On the CFD side, the HERO-SGBT outlet, which represents the main inlet surface for the CFD pool environment, is modelled adopting an imposed mass flow inlet condition. At the FPS inlet, instead, an imposed velocity condition is applied: the needed information is provided by the RELAP5 calculation at each time step. According to [14], defining the velocity distribution, it is one of the most practical ways to impose a mass flow rate at an outlet section; in addition, this assumption also allows for addressing possible backflow conditions which may appear in the numerical analysis owing to oscillations caused by the abrupt changes in the imposed Argon mass flow and was consequently selected in the present application. Eventually, at the top of the pool, a pressure inlet condition is applied. This was necessary in order to provide a suitable pressure value at the inlet and outlet sections which, after each internal iteration, provide these values to RELAP5.

On the RELAP5/Mod3.3 side, instead, the fluid dynamic coupling with the CFD domain is obtained by mean of Time-Dependent Volumes and single junctions. At each time step, the CFD code updates the pressure and temperature information in these volumes, thus providing RELAP with suitably updated boundary conditions.

Figure 3 resumes the thermal-hydraulic boundary conditions for the CFD side of the coupled calculation.

The coupled application performed by UniPi in Ref. [14] was here furthermore updated with the introduction of thermal boundaries between the CFD and the STH domain for the most relevant heat structures of the internal loop. This operation was performed in order to provide the coupled code with the capability to simulate the thermal stratification phenomena observed in the experimental results inside the pool. In particular, considering the results of a parallel work performed at the University of Pisa focusing on the prediction of this phenomenon in a CFD stand-alone application [22], heat transfer was assumed occurring through the thermal structures of the FPS and of the Fitting volume providing interesting results, the same surfaces are thus again considered for the present coupled calculation. During nominal operation conditions, the pool is in fact heated through these surfaces by the hot fluid flowing inside the CIRCE-loop; during the simulated accident, instead, more complex phenomena occur and heat transfer in both directions may be obtained as clearly highlighted later in this paper. The thermal coupling is achieved adopting an imposed heat flux condition, whose value is calculated by the CFD code, for the RELAP5 domain; the STH code instead provides the CFD domain with the corresponding wall temperature distribution: at each iteration, a check on the supplied heat is performed, assuring the energy balance.

The semi-implicit approach was instead adopted for the time-advancement scheme; the flow chart in Figure 4 reports the main steps of this procedure. In the reported picture UCFD and USTH represent the input vectors for the CFD domain and STH code, respectively; YCFD and YSTH are instead the output vectors; the Φ operator resumes instead all the internal operations occurring during the processing phase of each code. Eventually, the n apex refers to the current time step, while the k one refers instead to the current internal iteration.
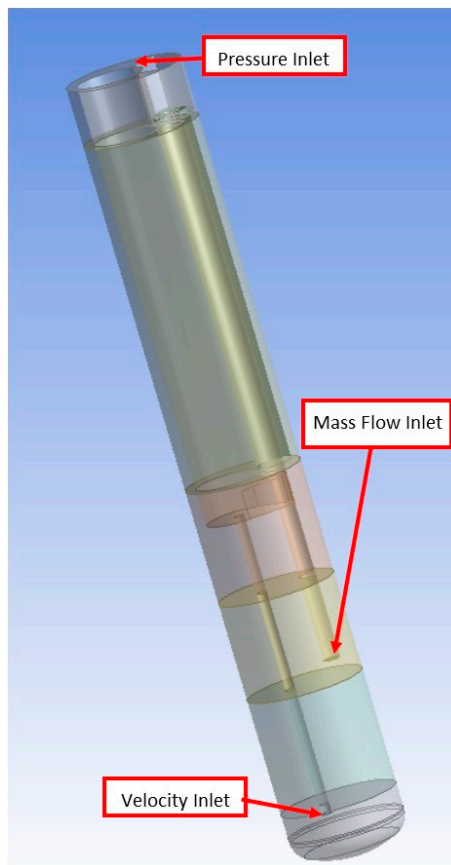
**Figure 3.** Computational fluid dynamics (CFD) domain boundary conditions.
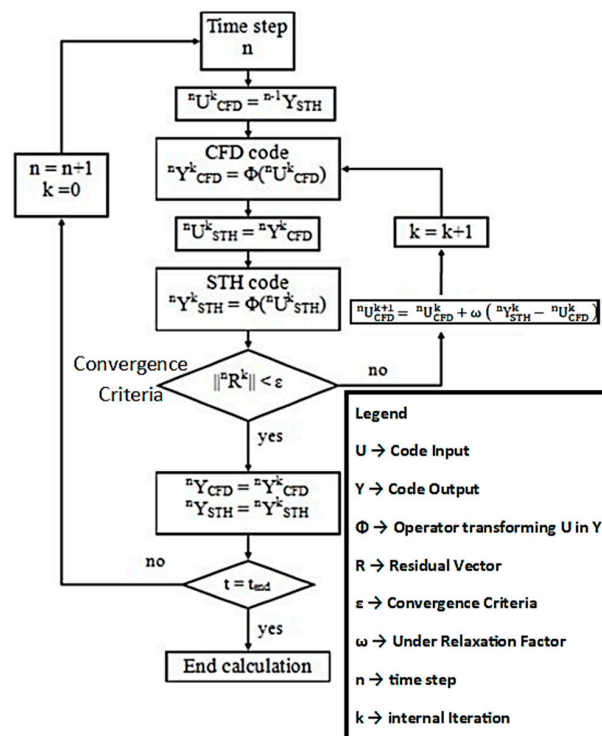


**Figure 4.** Time-advancing scheme.

Each time-step is solved iteratively: several internal iterations are performed in order to achieve a suitable matching between the predictions of the CFD and STH codes at the thermal and fluid-dynamic boundaries. In particular, CFD firstly performs its calculation providing RELAP5 with updated values for pressures, mass flow and heat fluxes ($Y_{CFD}$). RELAP5 subsequently performs its calculation considering the updated boundary conditions ($U_{STH} = Y_{CFD}$) and returns to the CFD code the updated boundary conditions ($Y_{STH}$) to be compared with the previous ones. If the resulting changes are sufficiently small (i.e., the obtained residual R is small), the calculation moves to the following time-step; if not, a new internal iteration starts and the calculation for the current time-step is repeated until the convergence criteria are met.

An under-relaxation factor of 0.5 was introduced for all the transferred quantities in order to increase the stability of this coupled application.

The coupled calculation was performed starting from initial steady-state conditions obtained as a result of stand-alone calculations of the CFD and STH domains and adopting an iterative procedure. After each calculation, the relevant exchanged properties were calculated and provided as boundary condition for the other code until a defined convergence criterium was achieved.

Nevertheless, as suggested in [23], the initial conditions of the presently considered PLOFA experiment probably did not completely achieve steady-state yet. As a consequence, in order to better reproduce the temperature distribution in the pool at the beginning of the experiment, the outlet temperature of HERO-SGBT was slightly increased with respect to the measured values and maintained constant during the initial iterative process, without taking into account the STH prediction. This assumption allowed predicting suitable initial conditions for the temperature calculated at the FPS inlet and for the fluid allocated in the bottom part of the pool also providing a good initial estimation for the mass flow rates and the pressure fields at the STH/CFD interfaces.

After the first time-step of the coupled calculation, the temperature imposed at the inlet of the domain CFD (at the HERO-SGBT outlet) becomes equal to the one actually calculated by the RELAP5 domain, granting a proper evolution in time of the considered phenomenon.

## 3. Results and Discussion

In this section, a comparison between the numerical results and the experimental data is presented, for a comparison with results provided by a STH code stand-alone calculation the reader is referred to [24].

Figure 5 shows the comparison between the measured and the calculated mass flow rate at the inlet section of the hot leg; a qualitative trend of the injected Argon mass flow rate is also reported as reference. As it can be observed, the calculated trend predicts very well the measured data and provides a good matching also for the final part of the considered time-frame. Only small variations in the predicted trends are expected for later times since no changes in the imposed operating conditions occur anymore.

The calculated trends do not reproduce the oscillating behaviour observed experimentally, predicting a smoother trend. The authors speculate that could be due to instantaneous fluctuations of the injected Argon mass flow rate, not sampled by the measurement system which may impact relevantly on the resulting LBE mass flow rate. Argon is in fact injected in order to enhance the natural circulation capabilities, affecting the pressure head at the bottom end of the hot leg and, as observed during the performed calculations, even small fluctuations of pressure at the two ends of the internal loop may induce relevant changes in the predicted LBE mass flow rate. Another possible cause of the observed mismatching may be related to the presence of entrapped air pockets (see, e.g., Ref. [25]) in the vicinity of the nozzle. This way, Argon injection may undergo cycles in which it is first accumulated, thus resulting in a decrease in the amount provided to the loop and a consequent decrease of the mass flow rate, and subsequently released in mass resulting in the experimentally observed peaks. In this case, the investigation of this phenomenon would require a detailed analysis of the injection system, also requesting the adoption of dedicated correlations, that cannot simply be implemented in

the STH code. Eventually, as also discussed in Ref. [26] the observed mismatching could also be due to unavoidable approximations introduced by correlations of the adopted models resulting unsuitable to perfectly reproduce two-phase flows characterized by relevant amounts of transported incondensable gases. Given the number of uncertainties, both on the experimental and numerical side, the obtained results can be considered a good prediction of the observed phenomenon.
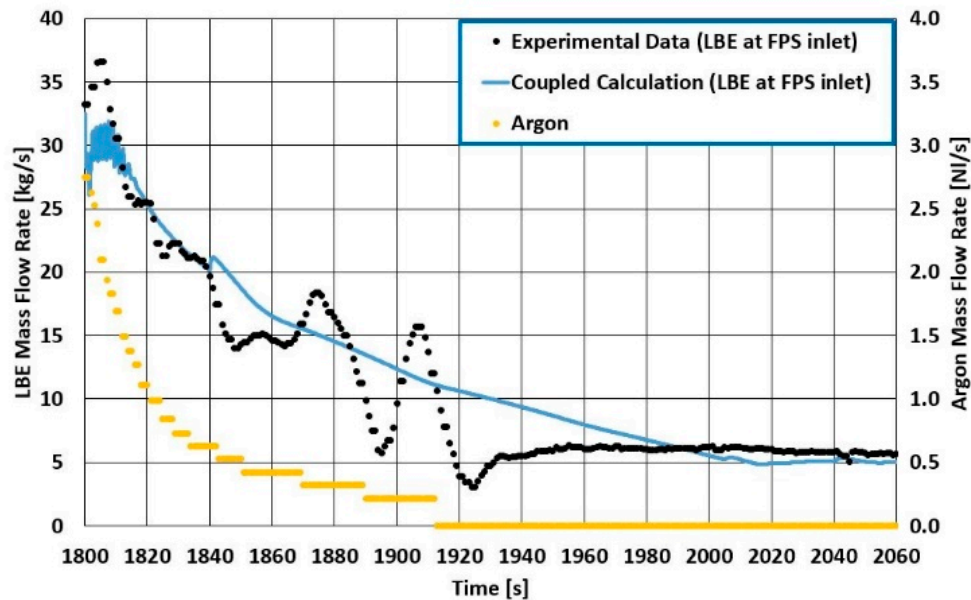


**Figure 5.** Comparison of the measured and calculated Lead Bismuth Eutectic (LBE) mass flow rates at the Fuel Pin Simulator (FPS) inlet section.

Figure 6 reports instead the comparison between the measured and calculated temperature trend at the inlet and outlet sections of the FPS. As it can be observed, a good prediction is again obtained. In particular, especially during the first part of the reported time interval the predicted outlet temperature matches fairly well the measured trend. Again, for later times, a smoother trend is predicted, in accordance with the predicted mass flow rate. In particular it must be observed that the outlet temperature underestimation occurring between time levels 1920 and 2000 s is due to the overprediction of the LBE mass flow rate in the corresponding leg during the same interval. This can be clearly observed comparing the trends reported in Figures 5 and 6.
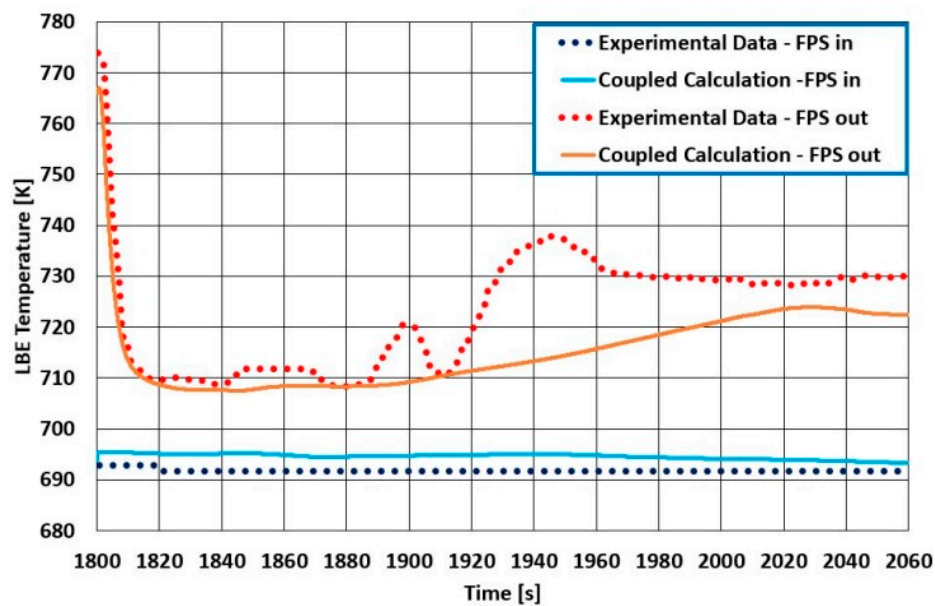
**Figure 6.** Comparison of the measured and calculated LBE temperatures at the FPS inlet and outlet sections.

It is also worth highlighting the thermal interactions occurring between the LBE flowing inside the FPS and the one inside the pool. In fact, during the time interval preceding the beginning of the PLOFA test, heat transfer is predicted to occur from the FPS to the pool; after a few seconds, instead, heat transfer occurs from the pool to the FPS. This is clearly shown in Figure 7, which reports the trend of the predicted heat flux in correspondence of the wall in the top section of the FPS. In the reported figure, a positive heat flux refers to power entering the pool from the FPS, a negative one is instead connected with power exiting the pool towards the FPS region.

This is due to the large differences in the thermal inertia of the two systems. While the fluid in the FPS rapidly becomes colder due to the lack of heating provided by the rods, the one in the pool, consisting in several tons of LBE, cools down following a relevantly slower transient. For a more accurate analysis of the observed phenomena the reader is also be referred to [27]. The impact of this heat transfer on the observed phenomena is relevant. In fact, during the steady-state conditions preceding the PLOFA test the observed heat contributes to the occurring of the observed thermal stratification phenomena; during the postulated PLOFA instead, it contributes in relevantly increasing the temperature inside the FPS, resulting in a total increase of about 20 °C with respect to the one that would be obtained in case of adiabatic FPS walls. In fact, in front of the 20 kW provided by the FPS at the end of the transient, the power provided through the considered walls also reaches 5 kW, thus relevantly contributing to the global energy balance of the FPS component. Though no comparison between the predicted and measured heat flux distributions is possible, the observed good matching between the measured and calculated outlet temperature trends suggests that the adopted coupling application managed to suitably reproduce the involved phenomena.
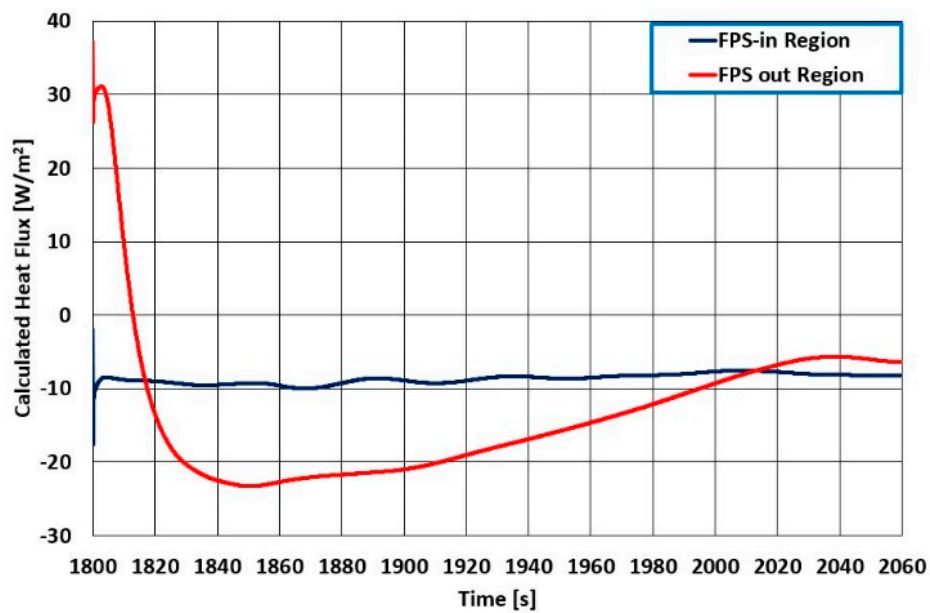
**Figure 7.** Calculated heat flux trend for the walls in correspondence of the top section of the FPS.

Thanks to the presence of a CFD domain, the coupled application also allows reproducing interesting distributions for some of the relevant properties.

In particular, it is possible to reproduce the path lines followed by the fluid exiting the HERO steam generator and entering the FPS. Figures 8 and 9 report these trends for two selected time levels; the former refers to the conditions at the beginning of the PLOFA transient (1800 s) while the latter reproduces the situation after 4 min from the beginning of the transient (2040 s).
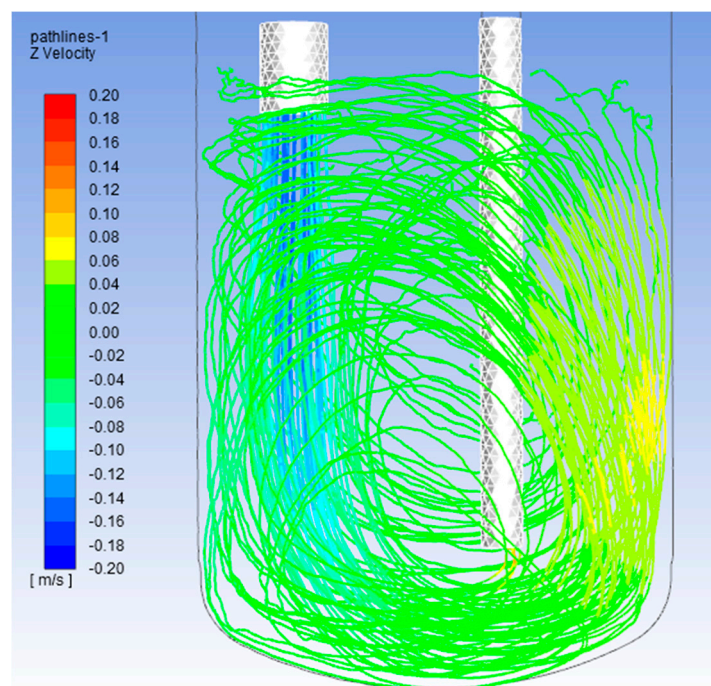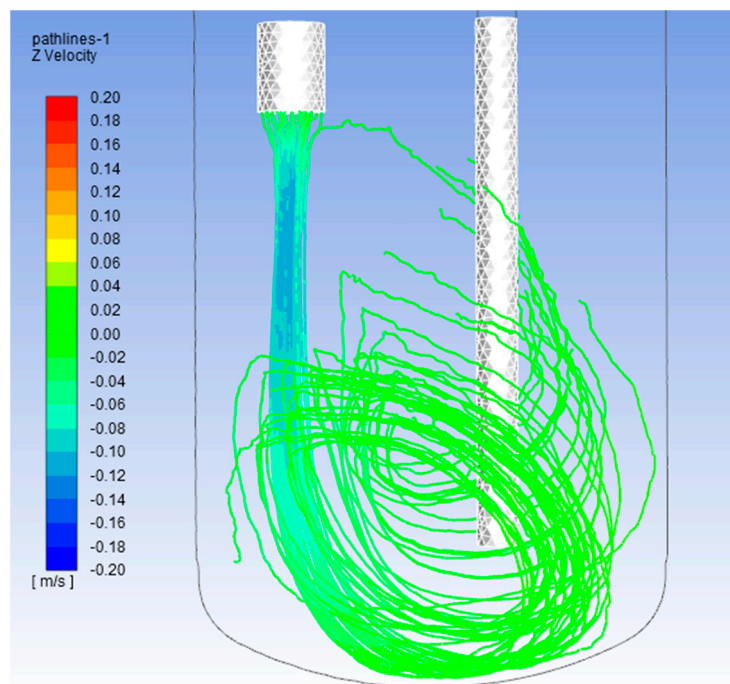


**Figure 8.** Pathlines for the fluid exiting the HERO steam generator and entering the FPS for t = 1800 s.

It is worth noticing that, because of the relevant change in the calculated LBE mass flow rates inside the pool, also the flow conditions in the bottom part of the pool changed consistently.

In particular, at the beginning of the transient, the large inertia forces resulting from the higher LBE mass flow rate at the HERO-SGBT implies a large recirculation region at the bottom of the pool inducing a relevant temperature mixing. As a consequence, only limited temperature variations should be experienced at the FPS inlet section (see also Figure 6).

On the other hand, after the decrease of the calculated mass flow rate occurring in the first minutes of the transient, the recirculation region becomes definitively smaller. This implies a sort of shortcut for the fluid exiting from the HERO-SGBT, which enters the FPS. In fact, the flow no more undergoes a strong mixing with the fluid in the pool, maintaining a temperature closer to the one predicted at the outlet of the steam generator. This phenomenon may be responsible for the predicted temperature decrease at the inlet of the FPS occurring in correspondence of the time interval in which the lower mass flow rates are predicted (1960–2060 s in Figure 6).



**Figure 9.** Pathlines for the fluid exiting the HERO steam generator and entering the FPS for t = 2040 s.

Figure 10 reports the temperature distribution calculated on a selected longitudinal section of the pool; the thermal stratification phenomenon also observed experimentally can be clearly noted, suggesting that the adopted coupled application is suitable for predicting the addressed experimental conditions. Due to the cited uncertainties in the initial conditions, the difficulties in performing experiments involving LBE and the intrinsic uncertainties of the measurements a quantitative comparison of measured and calculated values can be hardly performed. The calculated local temperature values differ from the measured of about 5–10 °C; nevertheless, the qualitative trend was captured. In addition, similar cooling rates were observed, suggesting once again that the adopted method seems suitable for the prediction of the involved phenomena.
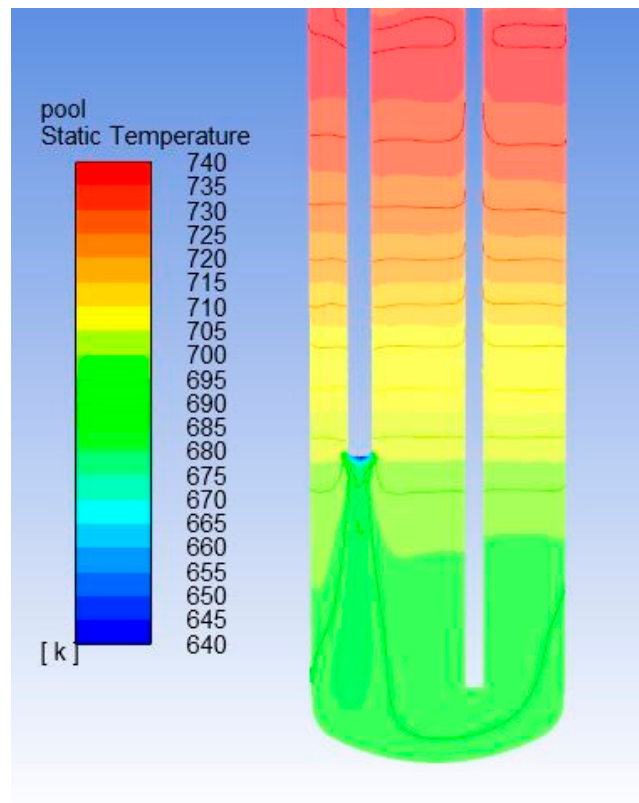
**Figure 10.** Calculated temperature distribution at the bottom of the pool for t = 2060 s.

### 4. Conclusions

In the present paper, the preliminary results of a coupled STH/CFD application involving the CIRCE-HERO facility were reported.

The facility represents a complicated thermal-hydraulic system which involves two-phase flow, non-condensable gas transport and flow conditions in an intrinsically three-dimensional environment. These characteristics make a stand-alone approach of the available modelling techniques hardly reliable presenting aspects that may impair the predicting capabilities of both STH and CFD codes.

As a consequence, a coupled STH/CFD application represents the best option for obtaining a suitable representation of the selected operating conditions. The computational domain was subdivided into several parts and each region was assigned to the code that could better represent its phenomena. The regions were consequently connected in order to allow mass and heat transfer between the various domains.

The obtained results suggested that coupled applications have promising capabilities in predicting the observed phenomena. A good matching between the measured and calculated trends was obtained for thetemperature distributions; for the mass flow rate instead, several hypotheses concerning the observed mismatching were formulated. Nevertheless, given all the uncertainties of the experimental setup, the obtained results may be considered as a good prediction of the experimental data. The coupled approach also allowed to observe and highlight the interesting phenomena occurring inside the pool. In particular, changes in the direction along which heat is transferred between the pool and the FPS were here clearly spotted and the pathlines distribution suggested possible explanations for the observed phenomena.

The performed work represents a valuable benchmark for the next applications to be developed at the University of Pisa as it highlighted both capabilities and weaknesses of the selected approach. In particular, the improved capabilities and the quality of the results provided by the addressed coupled STH/CFD code with respect to the STH stand-alone application seem worth the required

additional modelling and computational cost. The lessons drawn during the present application will be considered in order to refine and improve the presently adopted coupled STH/CFD approach in view of applications in future works. The modelling and discretizing approach adopted in the present work obviously has common characteristics with some of the referred papers thus suggesting that the considered technique may be approaching a sufficiently mature status. Since most of the presently referred applications were performed in the frame of the nuclear field, it is a common interest that this approach is considered suitable by licensing agencies. The development of Best Practice Guidelines to be adopted in coupled STH/CFD applications could be a sound strategy for paving the way for this achievement; the present paper thus calls the scientific community to pursue this common effort.

**Author Contributions:** Investigation and Formal Analysis; P.A.; writing original draft, writing, reviewing and editing; P.A., G.F., M.M., F.N., M.D.; project administration and supervision; F.N. All authors have read and agreed to the published version of the manuscript.

**Conflicts of Interest:** The authors declare no conflict of interest.

## References

1. Iamele, M.; (SCKCEN, Mol, Belgium). MYRRHA Technical Description. Rev. 1.6. SCKCEN/1148931. Tech. rep, Internal report. 2014.

2. *IAEA Design Features and Operating Experience of Experimental Fast Reactors*; IAEA Nuclear Energy Series NO. NP-T-1.9; International Atomic Energy Agency: Vienna, Austria, 2013.

3. Pucciarelli, A.; Barone, G.; Forgione, N.; Galleni, F.; Martelli, D. NACIE-UP post-test simulations by CFD codes. *Nucl. Eng. Des.* **2020**, *356*, 110392. [CrossRef]

4. Toti, A.; Vierendeels, J.; Belloni, F. Extension and application on a pool-type test facility of a system thermal-hydraulic/CFD coupling method for transient flow analyses. *Nucl. Eng. Des.* **2018**, *331*, 83–96. [CrossRef]

5. Toti, A. Development and Validation of a System Thermal-Hydraulic/ CFD Codes Coupling Methodology for Multi-Scale Transient Simulations of Pool-Type Reactors. Ph.D. Thesis, Ghent University, Ghent, Belgium, 2018. Available online: http://hdl.handle.net/1854/LU-8602537 (accessed on 10 October 2020).

6. Toti, A.; Vierendeels, J.; Belloni, F. Coupled system thermal-hydraulic/CFD analysis of a protected loss of flow transient in the MYRRHA reactor. *Ann. Nucl. Energy* **2018**, *118*, 199–211. [CrossRef]

7. Toti, A.; Vierendeels, J.; Belloni, F. Improved numerical algorithm and experimental validation of a system thermal-hydraulic/CFD coupling method for multi-scale transient simulations of pool-type reactors. *Ann. Nucl. Energy* **2017**, *103*, 36–48. [CrossRef]

8. Grishchenko, D.; Jeltsov, M.; Kööp, K.; Karbojian, A.; Villanueva, W.; Kudinov, P. The TALL-3D facility design and commissioning tests for validation of coupled STH and CFD codes. *Nucl. Eng. Des.* **2015**, *290*, 144–153. [CrossRef]

9. Jeltsov, M.; Kööp, K.; Kudinov, P.; Villanueva, W. Development of a domain overlapping coupling methodology for STH/CFD analysis of heavy liquid metal thermal-hydraulics. In Proceedings of the NURETH-15, Pisa, Italy, 12–17 May 2013.

10. Forgione, N.; Angelucci, M.; Ulissi, C.; Martelli, D.; Barone, G.; Ciolini, R.; Tarantino, M. Application of RELAP5/Mod3.3—Fluent coupling codes to CIRCE-HERO. *J. Phys. Conf. Ser.* **2019**, *1224*, 012032. [CrossRef]

11. Martelli, D.; Forgione, N.; Barone, G.; di Piazza, I. Coupled simulations of the NACIE facility using RELAP5 and ANSYS FLUENT codes. *Ann. Nucl. Energy* **2017**, *101*, 408–418. [CrossRef]

12. Angelucci, M.; Martelli, D.; Forgione, N.; Tarantino, M. RELAP5 STH and Fluent CFD Coupled Calculations of a PLOHS + LOF Transient in the HLM Experimental Facility CIRCE. In *Computational Fluid Dynamics (CFD) and Coupled Codes; Nuclear Education, Public Acceptance and Related Issues*; American Society of Mechanical Engineers: Shanghai, China, 2017; Volume 8, p. V008T09A045.

13. Angelucci, M.; Martelli, D.; Barone, G.; di Piazza, I.; Forgione, N. STH-CFD Codes Coupled Calculations Applied to HLM Loop and Pool Systems. *Sci. Technol. Nucl. Install.* **2017**, *2017*, 1–13. [CrossRef]

14. Zwijsen, K.; Martelli, D.; Breijder, P.A.; Forgione, N.; Roelofs, F. Multi-scale modelling of the CIRCE-HERO facility. *Nucl. Eng. Des.* **2019**, *355*, 110344. [CrossRef]

15. Galleni, F.; Barone, G.; Martelli, D.; Pucciarelli, A.; Lorusso, P.; Tarantino, M.; Forgione, N. Simulation of operational conditions of HX-HERO in the CIRCE facility with CFD/STH coupled codes. *Nucl. Eng. Des.* **2020**, *361*, 110552. [CrossRef]

16. Lorusso, P.; Pesetti, A.; Tarantino, M.; Narcisi, V.; Giannetti, F.; Forgione, N.; del Nevo, A. Experimental analysis of stationary and transient scenarios of alfred steam generator bayonet tube in circe-hero facility. *Nucl. Eng. Des.* **2019**, *352*, 110169. [CrossRef]

17. Lorusso, P.; Pesetti, A.; Barone, G.; Castelliti, D.; Caruso, G.; Forgione, N.; Giannetti, F.; Martelli, D.; Rozzia, D.; van Tichelen, K.; et al. MYRRHA primary heat exchanger experimental simulations on CIRCE-HERO. *Nucl. Eng. Des.* **2019**, *353*, 110270. [CrossRef]

18. Zhang, K. The multiscale thermal-hydraulic simulation for nuclear reactors: A classification of the coupling approaches and a review of the coupled codes. *Int. J. Energy Res.* **2020**, *44*, 3295–3315. [CrossRef]

19. Roelefs, F. *Thermal Hydraulics Aspects of Liquid Metal Cooled Reactors*; Woodheat Publishing: 2019; ISBN 978-0-08-101981-8. Available online: https://www.elsevier.com/books/thermal-hydraulics-aspects-of-liquid-metal-cooled-nuclear-reactors/roelofs/978-0-08-101980-1 (accessed on 10 October 2020).

20. Pesetti, A.; Forgione, N.; Narcisi, V.; Lorusso, P.; Giannetti, F.; Tarantino, M.; (ENEA, Roma, Italia); del Nevo, A. *ENEA CIRCE-HERO Test Facility: Geometry and Instrumentation Description*, Report ENEA CI-I-R-343; Internal report. 2018.

21. Lorusso, P.; Tarantino, M.; Polazzi, G.; Sermenghi, G. *D4.4 CIRCE-HERO PLOFA Experiment*. SESAME Report D4.4 Issued on 22/01/2019 by ENEA. Available online: https://ec.europa.eu/research/participants/documents/downloadPublic?documentIds=080166e5c126cf2c&appId=PPGMS (accessed on 10 October 2020).

22. Buzzi, F.; Pucciarelli, A.; Galleni, F.; Tarantino, M.; Forgione, N. Analysis of the thermal stratification phenomena in the CIRCE-HERO facility. *Ann. Nucl. Energy* **2020**, *141*, 107320. [CrossRef]

23. Narcisi, V.; Giannetti, F.; del Nevo, A.; Tarantino, M.; Caruso, G. Post-test simulation of PLOFA transient test in the CIRCE-HERO facility. *Nucl. Eng. Des.* **2019**, *355*, 110321. [CrossRef]

24. Moscardini, M.; Galleni, F.; Pucciarelli, A.; Forgione, N.; Martelli, D. Numerical analysis of the CIRCE-HERO PLOFA scenarios. *Appl. Sci.* **2020**, submitted for publication.

25. Balacco, G.; Fontana, N.; Apollonio, C.; Giugni, M.; Marini, G.; Piccinni, A.F. Pressure surges during filling of partially empty undulating pipelines. *ISH J. Hydraul. Eng.* **2018**. [CrossRef]

26. Issa, R.; Galleni, F. Mechanistic simulation of slug flow in vertical pipes using the one-dimensional two-fluid model. *Multiph. Sci. Technol.* **2015**, *27*, 229–245. [CrossRef]

27. Buzzi, F.; Pucciarelli, A.; Galleni, F.; Tarantino, M.; Forgione, N. Analysis of the temperature distribution in the pin bundle of the CIRCE facility. *Ann. Nucl. Energy* **2020**, *147*, 107717. [CrossRef]